Available online at www.sciencedirect.com
SCIENCE DIRECT®
Journal of Solid State Chemistry 177 (2004) 2772–2776
JOURNAL OF SOLID STATE CHEMISTRY
http://elsevier.com/locate/jssc

# Preparation and crystal structure of $Ba_2NF$

H. Seibel and T.R. Wagner*

*Department of Chemistry, Youngstown State University, One University Plaza, Youngstown, OH 44555-3663, USA*

Received 19 February 2004; received in revised form 13 April 2004; accepted 15 April 2004

**Abstract**

Single crystalline $Ba_2NF$ was prepared by heating a mixture of $KCuF_3$ and Ba metal to 900°C under dynamic flow of $N_2$, followed by slow cooling from the melt. Crystals of $Ba_2NF$ were dark violet in color and very air sensitive. X-ray diffraction experiments revealed that $Ba_2NF$ is isostructural with rocksalt-type BaO, and has space group $Fm\text{-}3\,m$ (No. 225) with cell parameter of $a = 5.6796(19)$ Å, $Z = 2$. X-ray data was collected on a Bruker SMART APEX 4k CCD Single Crystal Diffractometer at 100 K, using Mo($K_\alpha$) radiation. Structure refinement was carried out by full-matrix least squares on $F^2$ on all data, to give $R_1 = 0.0194$ (all data) and $wR_2 = 0.0433$ for 3 parameters and 23 independent reflections. The final position assignments were analyzed via bond valence sum calculations.
© 2004 Elsevier Inc. All rights reserved.

*Keywords:* Inorganic nitride-fluoride

## 1. Introduction

Compounds with compositions that can be derived from an oxide by replacement of two $O^{2-}$ ions with $N^{3-}$ and $F^-$ ions were referred to as pseudo-oxides by Andersson [1], in a paper reporting the preparation and structure characterizations of three phases in the Mg–N–F system. All three of the reported phases, L–$Mg_2NF$, $Mg_3NF_3$, and H–$Mg_2NF$ [1], have structures related to that of rocksalt-type MgO to various extents, depending largely upon the degree of anion ordering. The phase synthesized under ambient pressure conditions, L–$Mg_2NF$, has a tetragonal, anti-$LiFeO_2$-type structure due to ordering of N/F atoms along the *c*-axis. In the high-pressure H–$Mg_2NF$ phase, N/F atoms are not ordered, and the rocksalt-type structure of MgO is observed. The N/F atoms in $Mg_3NF_3$ also reportedly have an MgO-like arrangement, but one-fourth of the cations are missing relative to the MgO lattice. Most recently, a computational study [2] on the electronic properties of magnesium nitride fluorides appeared, in which $Mg_3NF_3$ and L–$Mg_2NF$ are predicted to be direct and indirect semiconductors, respectively. The implications of the paper point to potential applications for this class of materials in general.

Ehrlich et al. [3] reported the preparation of powder samples of $Ca_2NF$, $Sr_2NF$ and $Ba_2NF$. Based on a qualitative study using the Guinier X-ray powder diffraction method, they reported that all three of these compounds are isostructural with their analogous rocksalt-type oxides. Galy et al. [4] also reported a rocksalt structure for $Ca_2NF$. In previous studies, however, we prepared single crystalline samples of $Ca_2NF$ [5] and $Sr_2NF$ [6] and did not observe a rocksalt-type structure in either case. Instead, our $Ca_2NF$ sample was found to be isostructural with L–$Mg_2NF$, while $Sr_2NF$ can be described as a doubled rocksalt-type structure, due to ordering of N/F atoms along all three cell-axes. Very recently, we have prepared a $Ca_2NF$ phase which is isostructural with this doubled rocksalt-type $Sr_2NF$ phase (unpublished results). On the other hand, no ordering of N/F atoms was observed in our present study of $Ba_2NF$, and consequently an "ideal" rocksalt-type structure is reported. This study represents the first quantitative structural analysis for $Ba_2NF$.

*Corresponding author. Fax: +1-330-742-1579.
*E-mail address:* trwagner@cc.ysu.edu (T.R. Wagner).

0022-4596/$ - see front matter © 2004 Elsevier Inc. All rights reserved.
doi:10.1016/j.jssc.2004.04.026

## 2. Experimental

### 2.1. Sample preparation

An initial mixture consisting of a 3:1 mole ratio of Ba and $KCuF_3$ was placed in a Ni crucible, which was then placed into a silica tube that was sealed from air while allowing dynamic flow of inert gas. The $KCuF_3$ precursor was prepared according to the method reported by Langley et al. [7] The reaction mixture was first heated to 900°C under Ar and held there for 1 h, then was cooled to 200°C followed by reheating to 900°C under ultra-high-purity $N_2$ gas, and held for 4 h. The mixture was then cooled at a rate of 10°C/h to 200°C, and allowed to cool to room temperature for a total reaction time of approximately 4 days. Present in the final product mixture were very small and highly air sensitive dark violet crystals of $Ba_2NF$, which were invariably found embedded within colorless $BaF_2$ crystal matrices. For the crystal selected for final analysis, most of the surrounding $BaF_2$ matrix was cut away prior to X-ray data collection. The sample was sealed inside the tip of a glass capillary tube for protection from air during the experiment. Other crystal details are given in Table 1.

### 2.2. Structure determination

X-ray data were collected on a Bruker SMART APEX 4k CCD Single Crystal Diffractometer equipped with a normal focus, 2.4 kW sealed tube X-ray source (graphite monochromatized Mo$K_\alpha$ radiation, $\lambda = 0.71073$ Å) operating at 50 kV and 40 mA, and at a sample temperature of 100 K. The crystal-to-detector distance was 5.985 cm. The diffraction data was obtained by collection of 606 frames at each of three $\varphi$ settings, 0°, 120°, and 240°, using a scan width of 0.3° in $\omega$. At the end of the data collection, 50 initial frames were recollected to monitor crystal decay. The exposure time was 30 s/frame for both collections.

For the initial cell parameter determination, reflections were harvested from all 1868 frames of data for a minimum threshold of $I/\sigma$ of 1.0, using Bruker's SMART [8] program. Bruker's GEMINI [9] program revealed that most of the reflections in the resulting, array could be indexed as a single crystalline $Ba_2NF$ phase, while the remainder had a 6.2′ angstrom cubic cell pertaining to the $BaF_2$ matrix. Considering that no overlapping reflections were present, the orientation matrix corresponding to the $Ba_2NF$ crystal was then used to integrate all of the data in SAINT [8], where global refinement of the unit cell parameters was also performed to give the final values utilized in the subsequent structural analysis. An empirical absorption correction was next performed on the data files written by SAINT using SADABS [10], which also simultaneously corrected for other effects, such as absorption by the glass capillary. The optimal choice for space group was determined to be *Fm*-3*m* (No. 225) using Bruker's XPREP [11] program. Structure solution was obtained via direct methods using the SHELXS [11] program, and refinement was performed by full-matrix least squares on $F^2$ for all data using SHELXL [11]. The program SHELXP [11] was used to obtain the structure plot that appears in this paper. All refinement and crystal data is summarized in Table 1, and atomic coordinates and anisotropic and equivalent isotropic displacement parameters are listed in Table 2.

Table 1
Crystal data summary and refinement results for $Ba_2NF$

| | |
|---|---|
| Structural formula | $Ba_2NF$ |
| Formula weight | 307.69 |
| Color | Dark purple |
| Crystal size (mm) | $0.033 \times 0.024 \times 0.017$ |
| Space group | *Fm*-3*m* (No. 225) |
| $a$ (Å) | 5.6796(19) |
| $V$ (Å$^3$) | 183.21(11) |
| $Z$ | 2 |
| $\rho_{calc}$ (Mg/m$^3$) | 5.577 |
| $\lambda$ (Mo$K\alpha$) (Å) | 0.71073 |
| $\mu$ (mm$^{-1}$) | 21.146 |
| $\theta$ range for data collection (°) | 6.22 to 27.92 |
| Limiting indices | $-7 \leqslant h \leqslant 7$, $-7 \leqslant k \leqslant 7$, $-7 \leqslant 1 \leqslant 7$ |
| No. of reflections collected | 485 |
| No. of independent reflections | 23 ($R_{int} = 0.0595$) |
| No. of parameters | 3 |
| Refinement method | Full-matrix least squares on $F^2$ |
| Final $R$ indices [$I > 2\sigma(I)$] | $R_1(F)^a = 0.0194$, w$R_2(F^2)^b = 0.0433$ |
| Final $R$ indices (All Data) | $R_1(F)^a = 0.0194$, w$R_2(F^2)^b = 0.0433$ |
| Goodness-of-Fit on $F^2$ | 1.072 |
| Largest diff. peak and hole | 0.951 and $-0.481$ eÅ$^{-3}$ |

[a] $R_1(F) = \Sigma||F_o| - |F_c||/\Sigma|F_o|$ with $F_o > 4.0\sigma(F)$.
[b] $wR_2(F^2) = [\Sigma[w(F_o^2 - F_c^2)^2/\Sigma[w(F_o^2)^2]]^{1/2}$ with $F_o > 4.0\sigma(F)$, and $w^{-1} = \sigma^2(F_o)^2 + (W \cdot P)^2 + T \cdot P$, where $P = (\mathrm{Max}(F_o^2, 0) + 2F_c^2)/3$, $W = 0.0352$, and $T = 0.00$.

## 3. Results and discussion

### 3.1. Synthesis

In initial trials, a synthesis route similar to that used for the preparation of $Ca_2NF$ and $Sr_2NF$ crystals was followed, involving the reaction of the metal and metal fluoride under dynamic flow of $N_2$. Unlike the Ca–N–F and Sr–N–F cases however, a $Ba_2NF$ phase was never observed by this route. Instead, another Ba–N–F phase was prepared which appears to be a barium azide nitride fluoride material (unpublished results). The preparation of the $Ba_2NF$ phase was ultimately achieved using the previously described reaction of $KCuF_3$ with Ba metal under dynamic $N_2$ flow. Note that essentially the same product was obtained whether or not the mixture was heated in Ar prior to reaction in $N_2$. The final product

Table 2
Positional, Occupational, and Anisotropic[a] and Equivalent Isotropic[b] Displacement Parameters ($Å^2 \times 10^4$) for $Ba_2NF$ Crystal Refinement

| Atom | *Fd*-3*m* Site (Origin 2) | Site multiplicity | *x* | *y* | *z* | $U_{11}$ | $U_{23}$ | *U*(eq) |
|---|---|---|---|---|---|---|---|---|
| Ba(1) | 4b | 0.02192 | 0 | 0 | 0.5000 | 19(1) | 0 | 19(1) |
| [c]N(1) | 4a | 0.01042 | 0 | 0 | 0 | 22(4) | 0 | 22(4) |
| [c]F(1) | 4a | 0.01042 | 0 | 0 | 0 | 22(4) | 0 | 22(4) |

[a] The anisotropic thermal parameter is expressed as $\exp[-2\pi^2(h^2a^{*2}U_{11} + k^2b^{*2}U_{22} + l^2c^{*2}U_{33} + 2hka^*b^*U_{12} + 2hla^*c^*U_{13} + 2klb^*c^*U_{23})]$; $U_{11} = U_{22} = U_{33}$ and $U_{23} = U_{13} = U_{12}$.

[b] *U*(eq) is defined as one-third of the trace of the $U_{ij}$ orthogonalized tensor.

[c] N(1) and F(1) share the 4a site; site multiplicity values restrained to sum to 0.02083 (i.e., fully occupied); displacement parameters constrained to be equal.

mixture consisted of the $BaF_2$ and $Ba_2NF$ single crystals, mixed with a gray powder material that X-ray powder diffraction revealed to consist mainly of $BaF_2$, $Ba_3N_2$, and $Ba(N_3)_2$ powders. Copper metal was also present in abundance in the mixture; neither copper nor potassium-containing compounds were observed. The composition of the product mixture indicates that the primary reaction that occurred can be written,

$$KCuF_3 + 3Ba + 1/2N_2 \rightarrow Ba_2NF + BaF_2 + Cu + K\uparrow.$$

No potassium metal was observed amongst the final products, although its formation is strongly implied by the products that were (or were not) observed. Since the boiling point of potassium (i.e., about 770°C) is lower than the reaction temperature of 900°C, it evidently boiled off as it formed. Thus the reduction of $Cu^{2+}$ and $K^+$ ions coupled with the oxidation of Ba metal apparently facilitated the reduction of some $N_2$ molecules to $N^{3-}$ ions rather than mainly to azide ions, $N_3^-$, as observed in previous preparation attempts. This reaction could provide a simple route for the preparation of other single metal nitride fluorides as well. The presence of Ba–N phases detected in the product mixture can be accounted for by direct reaction between barium metal and nitrogen.

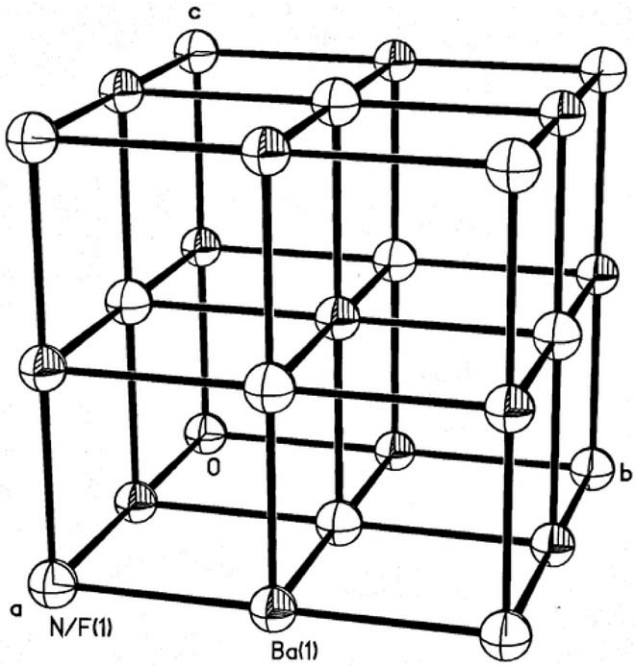


Fig. 1. Unit-cell structure plot (75% ellipsoids) for the final $Ba_2NF$ structure. N and F atoms share the anion site in a random fashion, with 50% occupancy for each atom.

### 3.2. Refinement

Data collection and refinement of the structure of the selected encapsulated $Ba_2NF$ crystal proceeded in a straightforward manner. The final cubic unit cell parameter obtained from the refinement was $a = 5.6796(19)$ Å, in close agreement with the value of $a = 5.691$ Å reported for $Ba_2NF$ in the qualitative powder X-ray diffraction study by Ehrlich et al. [3]. As reflected by the refinement parameters shown in Table 1, the structure analysis indicated decisively that our sample has the rocksalt-type structure, with no ordering of N and F atoms in the lattice. A plot of the final structure is shown in Fig. 1. Table 2 shows the occupational and displacement parameters. The shared N/F site was restrained to be fully occupied, and the occupancy of the barium site was refined merely to determine whether the final model has a refined composition that is consistent with the ideally expected one. This was found to be the case, as the final refined composition was $Ba_{4.2}N_{2.0}F_{2.0}$. (Note that the Ba occupancy factor is correlated with the anion site displacement parameter, and refined occupancy factors in general are usually not expected to represent quantitative compositions. Thus the refined 105% occupancy of the Ba site has no physical meaning, other than to show reasonable agreement with the proposed model.) Finally, the displacement parameters are within expected values.

### 3.3. Structure description and analysis

Not surprisingly, the crystal chemistries of $M_2NF$ for $M =$ Mg, Ca, Sr, and Ba are more complicated than the analogous oxides, due to the possibility of ordering of N & F atoms in the respective lattices. The fact that we

have never observed ideal rocksalt-type phases in the Ca–N–F & Sr–N–F systems seems mainly related to reaction and growth conditions rather than crystal chemical factors. For example, L–$Ca_2NF$ (5) and doubled cubic $Ca_2NF$ (unpublished results) were prepared in our lab under basically identical conditions that differed only in cooling rates.

A bond-valence sum analysis for our $Ba_2NF$ structure was performed using the program VALENCE [12], which computes the bond valence, $v_{ij}$, between two atoms $i$ and $j$ using the relation

$$v_{ij} = \exp[(R_{ij} - d_{ij})/0.37],$$

where $R_{ij}$ is a unitless empirical parameter characteristic of the atom pair forming the bond and $d_{ij}$ is the experimental bond length. The $R_{ij}$ values from Brese and O'Keeffe [13] of 2.47 and 2.19 for Ba–N and Ba–F bonds, respectively, were input into VALENCE for the computation, and the results are given in Table 3. Similarly to the cases reported previously for $Ca_2NF$ and $Sr_2NF$, the valence sum for Ba is quite underbonded compared to its ideal value of 2.0. This is in agreement with the observation by O'Keeffe and Hyde [14] that metal–oxygen bonds tend to be elongated (i.e. underbonded) in binary oxides with a high ratio (i.e., one or greater) of metal to nonmetal atoms, relative to the same bonds in ternary oxides. Furthermore, cation–cation interactions are expected to increase with cation size, so that one would expect $M$–O bonds to become increasingly underbonded in going from Ca to Sr to Ba compounds.

O'Keeffe [15] discussed this effect in binary oxides in terms of the ratio ($\Gamma$) of apparent (V′) to true (V) valences, where the apparent valence is the sum of calculated bond valences around the atom of interest, and the true valence is the (presumably) known oxidation state of the atom. Table 4 lists these ratios for the metal atoms in MO and various $M_2NF$ ($M$ = Mg, Ca, Sr, Ba) compounds, where these are listed in columns by structure type. Not surprisingly, the results indicate that the trend of increased underbonding with cation size tends to occur in the nitride–fluorides as well as the binary oxides. Of course, in order to more completely establish that cation–cation interactions, and therefore distances, are indeed anomalously long in $M_2NF$ compounds, one should ideally compare them to "normal" $M$–$M$ distances in nitride–fluoride compounds with lower metal/nonmetal ratios, similarly to comparison of cation–cation distances in binary vs. ternary compounds in analogous studies of oxides. [14,15] Unfortunately, no mixed-metal nitride–fluoride compounds are available at present for making such comparisons.

An exception to the trend of increased underbonding with cation size does appear in the rocksalt-type $M_2NF$ column of Table 4, where it is seen that $Sr_2NF$ actually has a significantly lower $\Gamma$ value than $Ba_2NF$. We have no explanation for this seeming anomaly. It is interesting to note, however, that the $\Gamma$ values are fairly consistent across rows for the different compositions/structure types of Mg, Ca and Ba compounds, while this is not the case for Sr, in which the $Sr_2NF$ values differ relatively significantly from each other and from SrO. Any error in the cell parameter for $Sr_2NF$ obtained from the Guinier powder diffraction study by Ehrlich et al. [3] is not likely to be large enough to account for the discrepancy. Also, as indicated in an earlier paper [6], their value of 5.38 Å is consistent with our doubled cubic cell parameters for $Sr_2NF$ of 10.692 and 10.766 Å for the two isostructural crystal-types observed in that study. The reason that the doubled cubic $Sr_2NF$ has a higher

Table 3
Bond valence sum results for $Ba_2NF$

| Bonds and bond lengths | Bond valences ($v_{ij}$) | | |
|---|---|---|---|
| | Ba(1) | N(1) | F(1) F(2) |
| Ba(1)–N(1) (2.8398 Å) | 0.368 (×3) | 0.368 (×6) | |
| Ba(1)–F(1) (2.8398 Å) | 0.173 (×3) | | 0.173 (×6) |
| $V_{ij} = \sum v_{ij}$ | 1.623 | 2.208 | 1.038 |

Table 4
Ratios of apparent to true valences ($\Gamma = V'/V$) for cations in MO and $M_2NF$ compounds

| | | Nitride–Fluoride (structure reference) | | | | | |
|---|---|---|---|---|---|---|---|
| Oxide | [a]$\Gamma$ | Tetragonal | [a]$\Gamma$ | Doubled cubic | [a]$\Gamma$ | Rocksalt | [a]$\Gamma$ |
| MgO | 0.98 | L–$M_{g2}NF$ (1) | 0.95 | | | | |
| CaO | 0.92 | L–$Ca_2NF$ (5) | 0.89 | [b]$Ca_2NF$ (unpub. results) | 0.93 | $Ca_2NF$ (3) | 0.89 |
| SrO | 0.88 | | | [c]$Sr_2NF$ (6) | 0.80 | $Sr_2NF$ (3) | 0.68 |
| BaO | 0.82 | | | | | $Ba_2NF$ (3) | 0.80 |
| | | | | | | $Ba_2NF$ (this study) | 0.81 |

[a] Computed using bond valence parameters from Brese and O'Keeffe [13], and bond lengths from indicated structure reference. For the oxides, bond lengths were taken from the Inorganic Crystal Structure Database, Nos. 52026, 52783, 28904, and 52278, respectively.
[b] Isostructural with $Sr_2NF$ (6); $a = 10.0215(8)$ Å.
[c] Calculated for the so called "BY" phase in Ref. 6.

Table 5
Ratios of apparent to true valences ($\Gamma = V'/V$) for anions in rocksalt-type $M_2$NF compounds

| N–F compound (Structure Ref.) | [a]$\Gamma$ for N | [a]$\Gamma$ for F |
|---|---|---|
| $Ca_2NF$ (3) | 0.82 | 1.10 |
| $Sr_2NF$ (3) | 0.58 | 0.98 |
| $Ba_2NF$ (this study) | 0.74 | 1.04 |

[a] Computed using bond valence parameters from Ref. [13], and bond lengths from indicated structure reference.

gamma value (although still low compared to SrO) than the rocksalt phase is explained by the fact that N and F are ordered in the doubled cubic phase, and so they do not share a position and are not constrained to have identical bond lengths as in rocksalt-type $Sr_2NF$. Consequently the Sr–N bonds are shorter (i.e. 2.58 Å) in this structure than the Sr–F bonds (i.e. 2.77 Å). Thus if the crystal data cannot account for the lower-than expected value of $\Gamma$ for Sr in $Sr_2NF$, the only other possibility would seem to be a discrepancy in the bond valence parameter $R_{ij}$ itself used for calculating the Sr–N bond valence.

Finally, note that relatively strong cation–cation interactions in $Ba_2NF$ could also explain the low apparent valence of 2.208 observed for nitrogen, as indicated in Table 3. It follows that since the metal atoms in $M_2$NF compounds are underbonded, then at least one of the anions (only nitrogen in this case) should be as well. Furthermore, a trend of decreasing bond valence sums for nitrogen would be expected in going from $M$ = Ca to Sr to Ba in rocksalt-type $M_2$NF. This is necessarily true for oxygen in the analogous MO compounds, as is evident from the $\Gamma$ ratios for the metal atoms listed in Table 4. Table 5 gives the corresponding values for the rocksalt-type nitride–fluorides. The $\Gamma$ ratio for nitrogen in $Ca_2NF$ is the highest, although there is again an exception at $Sr_2NF$, which has the lowest value. The fluorine atoms, on the other hand, all have $\Gamma$ ratios near their ideal value of one. Thus the $M$ to shared N/F bond length in each case is close to ideal for an $M$–F bond, whereas one might expect the constrained, or average, $M$–N/F bond length in the rocksalt structure to be between the $M$–N and $M$–F "ideal" bond lengths. We conclude that this is not the case due to $M$–$M$ repulsions, which inhibit the $M$–N/F bond lengths from becoming shorter despite the incentive for this to occur otherwise.

## 4. Summary

Single crystals in the Ba–N–F system have been prepared and structurally quantified for the first time. The phase isolated in this study was $Ba_2NF$, and was found to be isostructural with rocksalt-type BaO. The synthesis of the sample by the reaction of a ternary fluoride with Ba metal offers a possible route for the preparation of other inorganic nitride–fluorides.

## Acknowledgments

HS gratefully acknowledges summer support from NSF-REU Grant # 0097682. Purchase of the CCD X-ray diffractometer at Youngstown State University was supported in part through funding from NSF-CCLI Grant # 0087210, and from the Ohio Board of Regents Action Fund, Grant CAP-491.

## References

[1] S. Andersson, J. Solid State Chem. 1 (1970) 306.
[2] C.M. Fang, K.V. Ramanujachary, H.T. Hintzen, G. de With, J. Alloys Comp. 351 (2003) 72.
[3] P. Ehrlich, W. Linz, H. Seifert, Naturwissenschaften 58 (1971) 219.
[4] J. Galy, M. Jaccou, S. Andersson, C.R. Acad. Sci. Paris 272 (1971) 1657.
[5] R. Nicklow, T. Wagner, C. Raymond, J. Solid State Chem. 160 (2001) 134.
[6] T. Wagner, J. Solid State Chem. 169 (2002) 13.
[7] R.H. Langley, C.K. Schmitz, M.B. Langley, J. Chem. Ed. 61 (1984) 643.
[8] J.L. Chambers, K.L. Smith, M.R. Pressprich, Z. Jin, SMART Ver. 5.625 Program for Data Collection and SAINT-Plus Ver. 6.22 Data Processing for SMART System, Broker Analytical X-ray Instruments, Inc., Madison, WI, USA, 2001.
[9] Bruker AXS, GEMINI Ver. 1.02 Program for Indexing Twinned Crystals, Bruker Analytical X-ray Instruments, Inc., Madison, WI, USA, 2000.
[10] G.M. Sheldrick, SADABS Ver. 2.03 Software for Area Detector Absorptions and Other Corrections, Bruker Analytical X-ray Instruments, Inc., Madison, Wisconsin, USA, 2001.
[11] G.M. Sheldrick, SHELXTL-NT Ver. 6.10 Software Package for the Refinement of Crystal Structures, Bruker Analytical X-ray Instruments, Inc., Madison, Wisconsin, USA, 2000.
[12] C. Hormillosa, S. Healy, T. Stephan, VALENCE Ver. 2.00 Bond Valence Calculator Program, distributed by I.D. Brown, McMaster University, Ont. Canada, 1993.
[13] N.E. Brese, M. O'Keeffe, Acta Crystallogr. B 47 (1991) 192.
[14] M. O'Keeffe, B. Hyde, Nature 309 (1984) 411.
[15] M. O'Keeffe, Structure Bonding 71 (1989) 161.